ELSEVIER

Journal of Photochemistry and Photobiology A: Chemistry 90 (1995) 11–17

Journal of PHOTOCHEMISTRY AND PHOTOBIOLOGY A: CHEMISTRY

The absorption of pulsed CO_2 laser radiation by methylphosphine as a function of wavenumber, fluence, pulse duration, temperature, optical path length and pressure of absorbing and non-absorbing gases

J. Rak [a], J. Błażejowski [a], F.W. Lampe [b]

[a] *Department of Chemistry, University of Gdańsk, 80-952 Gdańsk, Poland*

[b] *Department of Chemistry, The Pennsylvania State University, 152 Davey Laboratory, University Park, PA 16802, USA*

Received 22 November 1994; accepted 7 February 1995

Abstract

The absorption of four lines (P12 (951.2 cm^{-1}) and R22 (977.2 cm^{-1}) (00°1–10°0 transition) and P36 (1031.5 cm^{-1}) and R20 (1078.6 cm^{-1}) (00°1–02°0 transition)) of a pulsed CO_2 laser by CH_3PH_2 was examined at various pulse energies, pulse durations, temperatures, optical path lengths and pressures of the compound and non-absorbing foreign gases. In addition, the low intensity IR absorption spectrum of methylphosphine was compared with high intensity absorption data relevant to all lines of the pulsed CO_2 laser. The experimental characteristics demonstrate non-linear features of the absorption phenomena and can be expressed analytically by a formula equivalent to an extended form of the phenomenological Beer–Lambert law. The importance of the results obtained for revealing general regularities governing the multiphoton absorption and the potential applications of CH_3PH_2 are indicated briefly.

Keywords: Absorption; CO_2 laser radiation; Methylphosphine; Phenomenological description

1. Introduction

Methylphosphine is one of the simplest phosphorus compounds and can potentially be formed from the interaction of simple hydrides of carbon and phosphorus (it was discovered in the atmospheres of Jupiter and Saturn and plays an important role in the transformations which take place in the atmospheres of these giant planets [1,2]). Three normal modes of the compound (namely ν_7 (977.6 cm^{-1}), ν_{13} (1016.9 cm^{-1}) and ν_6 (1091.9 cm^{-1})) [3] fall within the region of the emission of the CO_2 laser [4], which makes the CH_3PH_2 molecule a very convenient model for studying features of IR photochemistry and high intensity radiation spectroscopy. Methylphosphine can also be considered to be a source of phosphorus in the preparation of doped amorphous silicon hydrides or other materials of potential technological importance [5–7]. These reasons prompted us to investigate the ability of the compound to interact with the intense CO_2 laser photon field in order to extend our knowledge of the absorption phenomena (this is the subject of the present paper) and to reveal features of its IR photochemistry (this problem will be considered in one of our forthcoming articles).

Almost two decades of investigation on the absorption of CO_2 laser radiation have revealed that the phenomenological Beer–Lambert law, very useful in the description of absorption phenomena accompanying low intensity radiation, does not apply in prevailing high radiation density conditions [8–23]. It has been found that the absorption coefficient (cross-section), characteristic of a given wavenumber in both low and high [10,11,16] intensity absorption, depends on the fluence [9–12,14,17–19,21,23] and intensity [13] of the radiation, the pressure of the absorbing [9–12,14–16,18,21] and non-absorbing [16–19,21,22] entities, the temperature [18,20] and the optical path length [18,21] on interaction of a system with high power IR radiation. For a quantitative description of the photochemical processes initiated by such radiation, a knowledge of the amount of energy absorbed in any experimental condition is required. This necessitates finding an expression which relates the absorption to all parameters affecting it. In this paper, we propose a relationship based on the Beer–Lambert law, extended so as to reflect the effects of pressure, pulse energy, temperature and optical path length on the absorption process. Some aspects of this problem have been considered previously [16,18].

2. Experimental details

Methylphosphine was synthesized by the Crosbie and Sheldrick method [24] and was subsequently purified by

1010-6030/95/$09.50
SDI 1010-6030(95)04061-7

vacuum distillation. The identity of the product was confirmed by mass spectrometry. He (99.995%) (from Matheson) and N_2 (99.998%) (from Linde) were used as received. All gas mixtures were prepared using a Saunders–Taylor apparatus [25].

The source of IR radiation was a pulsed, transversely excited atmospheric (TEA) CO_2 laser (Lumonics, model 103-2). The central portion of the laser beam was stopped down to an area of 3 cm^2 by a metal aperture and attenuated, if necessary, by passing it through polyethylene sheets. Experiments were carried out at three different pulse lengths, achieved by varying the composition of the lasing gas mixture. As was revealed by Jang and Setser [26], for operation without N_2 ($He:CO_2:N_2 = 10.0:5.0:0.0$), the laser pulse is a 100 ns (full width at half-maximum (FWHM)) spike without any tail (short pulse). In the case of the lasing gas mixture with a composition of $He:CO_2:N_2 = 10.0:3.0:0.6$, a 100 ns initial spike is followed by a tail extended to 1.3 μs (approximately 45% of the energy is contained in the tail) (long pulse). We note, however, that the maximum energy output is reached if the composition of the lasing gas mixture is $He:CO_2:N_2 = 6.0:2.0:0.7$ [27] (regular pulse).

Absorption measurements were carried out in a stainless steel cell equipped with NaCl windows [28]. The incident pulse energy (E_0), the amount of energy transmitted by the empty cell (E_{empty}) and the amount of energy transmitted by the cell filled with a gaseous phase (E_{full}) were measured using a Gen-Tec (model ED-500) joulemeter. The absorption data are presented in terms of the fraction of energy absorbed (F)

$$F = \frac{E_{empty} - E_{full}}{E_0} = \frac{E_{abs}}{E_0} \quad (1)$$

the optical density (OD)

$$OD = \ln\left(\frac{1}{1-F}\right) \quad (2)$$

or the absorption cross-section (σ, in m^2 $molecule^{-1}$)

$$\sigma = \frac{OD}{LP} \quad (3)$$

where L denotes the optical path length, P is the pressure of the absorbing gas and E_{abs} is the amount of energy absorbed.

3. Results

The low intensity IR absorption spectrum of gaseous CH_3PH_2 in the region of the ν_7, ν_{13} and ν_6 fundamental vibrations [3], together with the absorption data of the CO_2 laser lines [4], is presented in Fig. 1. As can be seen, both sets of characteristics follow roughly the same trends, although the low intensity absorption cross-sections are twofold higher than the high intensity absorption cross-sections on average.

Figs. 2 and 3 demonstrate the optical density of neat CH_3PH_2 as a function of the pulse energy (fluence) for four laser lines and five pressures. Typical saturation-type dependences are observed for all laser lines and pressures

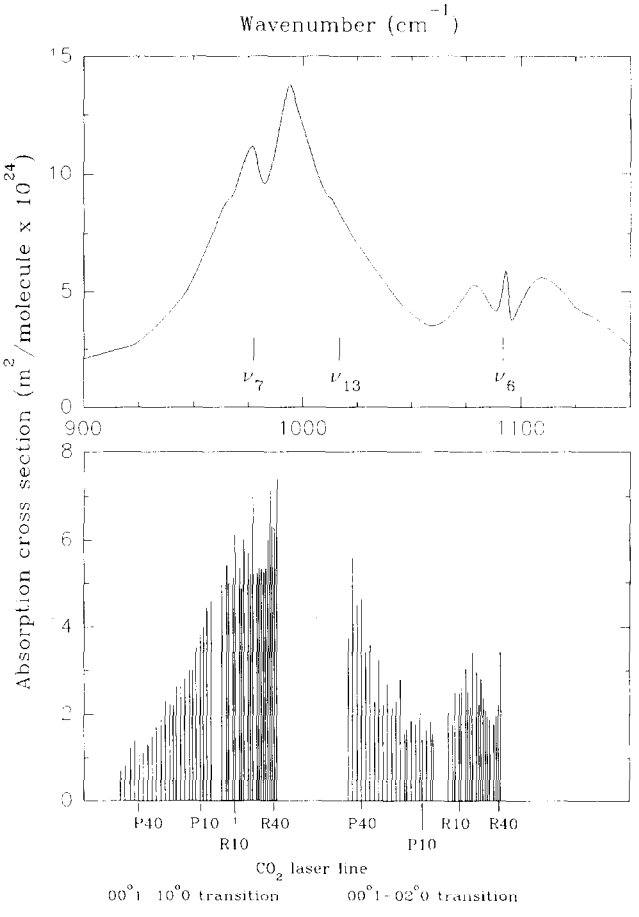

Fig. 1. Low intensity absorption cross-section (absorption spectrum) of CH_3PH_2 (pressure, 30 Torr) as a function of wavenumber (top graph) and high intensity absorption cross-section of the compound (pressure, 100 Torr) as a function of the CO_2 laser line (regular pulse) (bottom graph) at ambient temperature and 11.5 cm optical path length.

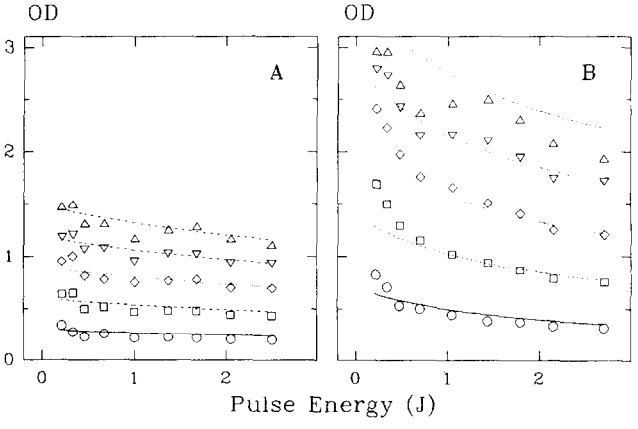

Fig. 2. Optical density vs. pulse energy at various pressures (Torr) of CH_3PH_2 (20 (○), 40 (□), 60 (◇), 80 (▽) and 100 (△)), ambient temperature and 11.5 cm optical path length (P12 (951.2 cm^{-1}) (A) and R22 (977.2 cm^{-1}) (B) lines of the 00°1–10°0 CO_2 laser transition (regular pulse)).

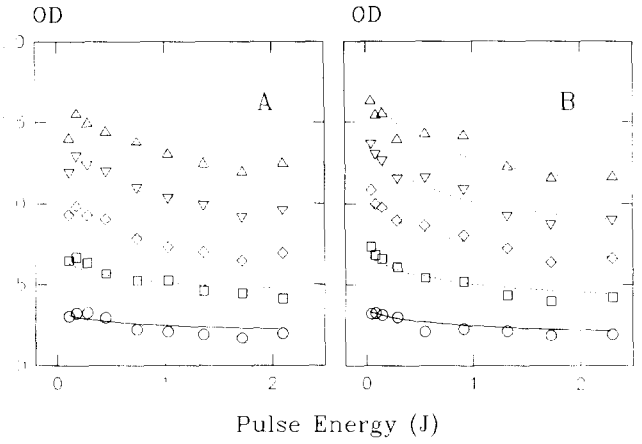

Fig. 3. Optical density vs. pulse energy at various pressures (Torr) of CH_3PH_2 (20 (○), 40 (□), 60 (◇), 80 (▽) and 100 (△)), ambient temperature and 11.5 cm optical path length (P36 (1031.5 cm^{-1}) (A) and R20 (1078.6 cm^{-1}) (B) lines of the 00°1–02°0 CO_2 laser transition (regular pulse)).

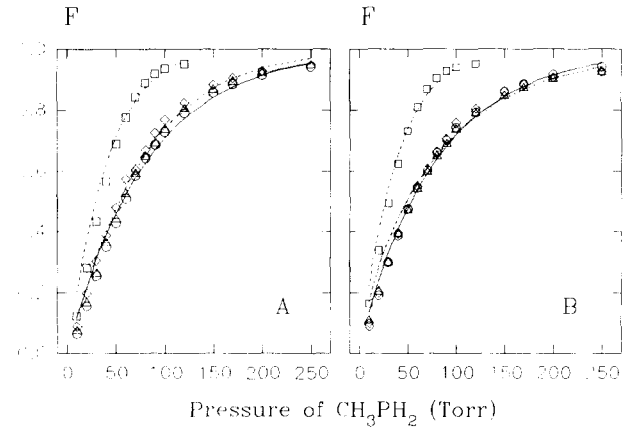

Fig. 4. Fraction of energy absorbed vs. pressure of CH_3PH_2 at ambient temperature and an optical path length of 11.5 cm (dependence for the short (A) and long (B) pulse). P12 (○) (951.2 cm^{-1}; $E_0 = 1.22$ (A) and 1.27 (B) J per pulse) and R22 (□) (977.2 cm^{-1}; $E_0 = 1.22$ (A) and 1.35 (B) J per pulse) demonstrate the absorption of the CO_2 laser lines corresponding to the 00°1–10°0 transition. P36 (◇) (1031.5 cm^{-1}; $E_0 = 0.77$ (A) and 0.89 (B) J per pulse) and R20 (△) (1078.6 cm^{-1}; $E_0 = 0.95$ (A) and 1.01 (B) J per pulse) demonstrate the absorption of the CO_2 laser lines corresponding to the 00°1–02°0 transition.

[9,12,18,29]. The effect is most pronounced for the R22 line which is absorbed most strongly (Fig. 2(B)).

The fraction of energy absorbed as a function of pressure appears to be very similar for short and long pulses (Fig. 4), although the amount of energy absorbed usually increases when the duration of the laser pulse increases [18]. If absorption is expressed in terms of the optical density and plotted against pressure, characteristic positive deviations from the Beer law are observed in the low pressure region and at short optical path lengths (Fig. 5) [16–18,21]. At higher pressures, however, the optical density starts to deviate in the opposite direction (negative deviations) (Fig. 5(B)). The latter effect often accompanies the absorption phenomena.

Figs. 6 and 7 demonstrate the enhancement of absorption in the presence of foreign gases (He and N_2). This effect is

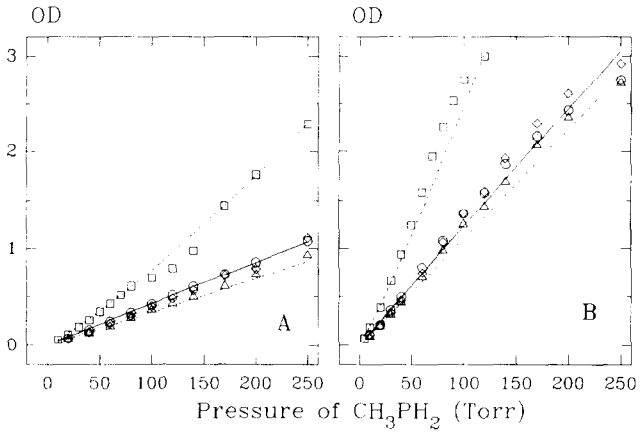

Fig. 5. Optical density vs. pressure of CH_3PH_2 at ambient temperature (dependence for 3.5 cm (A) and 11.5 cm (B) optical path length). P12 (○) (951.2 cm^{-1}; $E_0 = 1.71$ J per pulse) and R22 (□) (977.2 cm^{-1}; $E_0 = 1.72$ J per pulse) demonstrate the absorption of the CO_2 laser lines corresponding to the 00°1–10°0 transition. P36 (◇) (1031.5 cm^{-1}; $E_0 = 1.56$ J per pulse) and R20 (△) (1078.6 cm^{-1}; $E_0 = 1.73$ J per pulse) demonstrate the absorption corresponding to the 00°1–02°0 transition (regular pulse).

characteristic of the interaction of high intensity CO_2 laser radiation with matter [16,17,30].

Figs. 8 and 9 show the optical density of neat CH_3PH_2 vs. the optical path length for three temporal distributions of the laser pulse and four laser lines. The experimental characteristics show slight negative deviations from the Lambert law. This effect commonly accompanies the absorption of electromagnetic radiation.

Finally, Fig. 10 demonstrates the gradual increase in optical density with increasing temperature. The effect, although weak, seems to be specific for the absorption of high power CO_2 laser radiation [18,20].

4. Discussion

Figs. 2–10 show the absorption of methylphosphine in various conditions. As the latter are represented by the experimental parameters, i.e. pressure of the absorbing and non-absorbing (P_i) entities, optical path length, temperature (T) and incident pulse energy, the optical density or fraction of energy absorbed is a function of these. The search for an expression relating these quantities [16,18] was based on the phenomenological Beer–Lambert law [31]

$$OD = \epsilon PL \quad (4)$$

(where ϵ is the absorption coefficient expressed in cm^{-1} $Torr^{-1}$ (1 Torr = 133.322 N m^{-2}) characteristic of a given wavelength (wavenumber)), which well describes the absorption of low intensity radiation. It is evident from an examination of the experimental dependences (Figs. 2–10) that expression (4) can be applied for high radiation density conditions only if we make the absorption coefficient dependent on all five above-mentioned experimental parameters, namely P, P_i, E_0, L and T. Such a dependence must reflect an

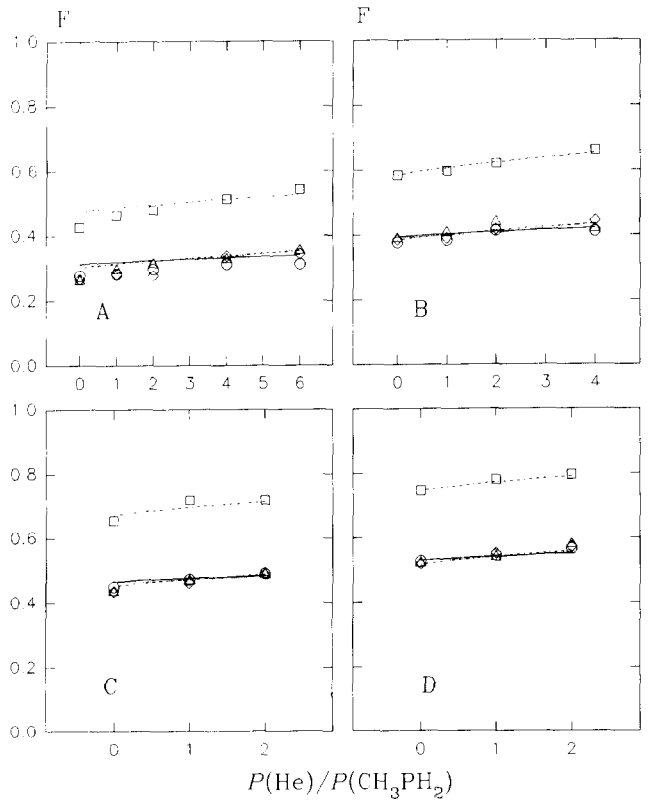

Fig. 6. Absorption of CO_2 laser radiation by CH_3PH_2 for P12 (951.2 cm^{-1}; $E_0 = 1.79$ J per pulse) (○) and R22 (977.2 cm^{-1}; $E_0 = 1.81$ J per pulse) (□) lines of the 00°1–10°0 transition, and P36 (1031.5 cm^{-1}; $E_0 = 1.27$ J per pulse) (◇) and R20 (1078.6 cm^{-1}; $E_0 = 1.28$ J per pulse) (△) lines of the 00°1–02°0 transition (regular pulse), in the presence of helium (A, B, C and D for 30, 40, 50 and 60 Torr of CH_3PH_2 respectively) at ambient temperature and 11.5 cm optical path length.

increase in the absorption coefficient with a decrease in E_0 (i.e. ϵ must reduce to the value of the low intensity absorption coefficient (ϵ_0) at $E_0 \rightarrow 0$) and, on the other hand, should describe a decrease in this coefficient with an increase in the incident pulse energy (the latter feature is demonstrated in Figs. 2 and 3). The simple relationship which takes into account both of these factors is similar to the equation of the Langmuir adsorption isotherm [30] (one of the simplest saturation-type dependences), namely

$$\epsilon = \epsilon_0 \frac{[1 + (E_0/E_c)A]}{[1 + (E_0/E_c)]} \tag{5}$$

where ϵ_0 and E_c are adjustable parameters (the meaning of ϵ_0 is described above and E_c was introduced to make E_0/E_c dimensionless) and A represents the term accounting for the influence of other experimental parameters on the absorption process. As the experimental results demonstrate, the optical density (or fraction of the energy absorbed) increases with an increase in the pressure of the absorbing (Figs. 4 and 5) and non-absorbing (Figs. 6 and 7) gases, which can be interpreted as a result of collisions. According to the kinetic theory of gases, the number of collisions is proportional to the product of the pressures of the colliding entities and to the square root of the temperature [31]. The pressure of the absorbing molecules already occurs in Eq. (4). We assume that the pressures of the gases affecting absorption are included in the term A (Eq. (5)) as the sum extending over all absorbing and non-absorbing entities, namely

$$A = \left(\frac{L}{L_0}\right)^a \left(\frac{T}{T_0}\right)^{1/4} \left\{ C \left[\frac{P}{P_0} \left(\frac{T}{T_0}\right)^{1/4} \right]^n + \sum_i C_i \left[\frac{P_i}{P_0} \left(\frac{T}{T_0}\right)^{1/4} \right]^{n_i} \right\} \tag{6}$$

The extent to which collisions affect the process was accounted for by introducing adjustable parameters of two categories, namely C (C_i) and n (n_i). If the influence of temperature on the process (Fig. 10) originates from collisions, we would expect the enhancement of the absorption to be proportional to the square root of T. Assuming that this effect can be ascribed equally to absorption and collision with these entities, we can share equally $T^{1/2}$ between two $T^{1/4}$ terms, where the term occurring before the braces in Eq. (6) reflects the part affiliated to the absorbing molecules and that after the pressures in Eq. (6) reflects the part relevant to the molecules which enhance absorption. Finally, we assume that the deviations from linearity of the optical density vs. optical path length dependences (Figs. 8 and 9) can be accounted

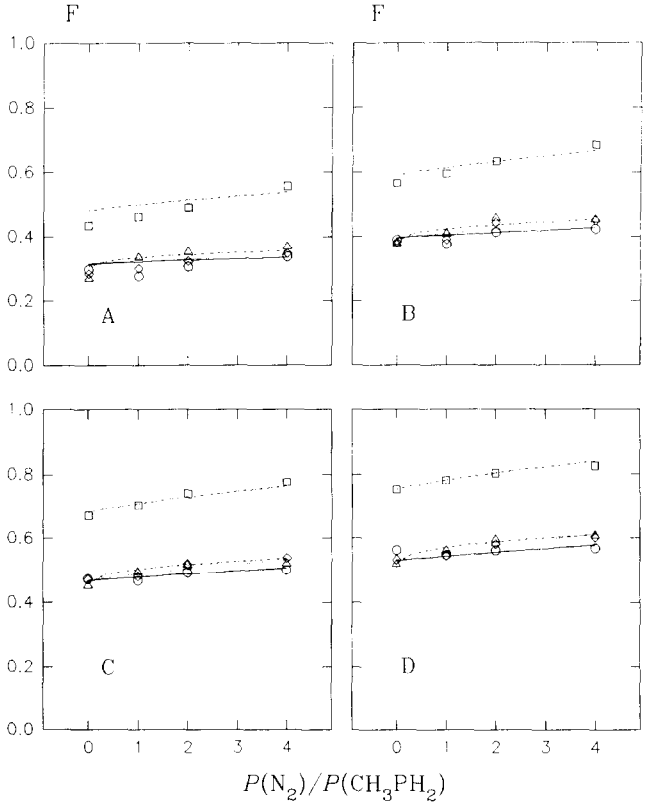

Fig. 7. Absorption of CO_2 laser radiation by CH_3PH_2 for P12 (951.2 cm^{-1}; $E_0 = 1.67$ J per pulse) (○) and R22 (977.2 cm^{-1}; $E_0 = 1.69$ J per pulse) (□) lines of the 00°1–10°0 transition, and P36 (1031.5 cm^{-1}; $E_0 = 1.19$ J per pulse) (◇) and R20 (1078.6 cm^{-1}; $E_0 = 1.20$ J per pulse) (△) lines of the 00°1–02°0 transition (regular pulse), in the presence of nitrogen (A, B, C and D for 30, 40, 50 and 60 Torr of CH_3PH_2 respectively) at ambient temperature and 11.5 cm optical path length.

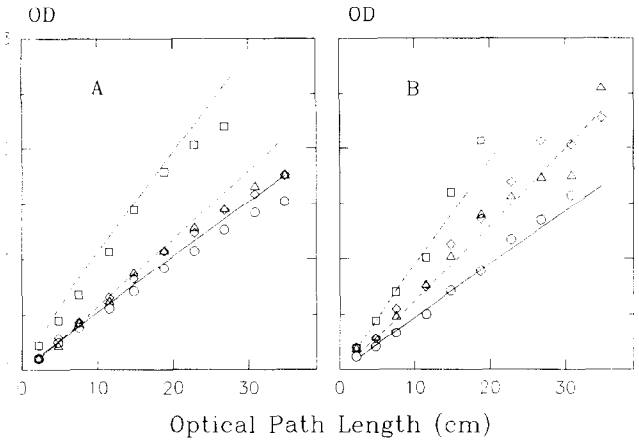

Fig. 8. Optical density of 50 Torr of CH_3PH_2 at ambient temperature vs. the optical path length for short (A) and long (B) pulses on absorption of the P12 (951.2 cm^{-1}; $E_0 = 1.36$ (A) and 1.66 (B) J per pulse) (○) and R22 (977.2 cm^{-1}; $E_0 = 1.33$ (A) and 1.75 (B) J per pulse) (□) laser lines of the 00°1–10°0 transition, and P36 (1031.5 cm^{-1}; $E_0 = 0.78$ (A) and 1.34 (B) J per pulse) (◇) and R20 (1078.6 cm^{-1}; $E_0 = 0.92$ (A) and 1.53 (B) J per pulse) (△) lines of the 00°1–02°0 transition.

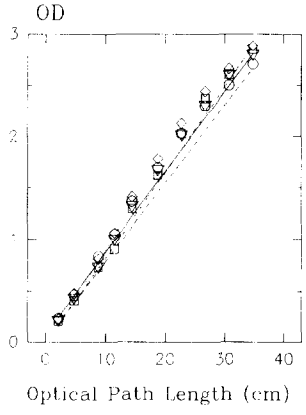

Fig. 9. Optical density vs. optical path length on absorption of the P12 (951.2 cm^{-1}; $E_0 = 1.65$ J per pulse; $P(CH_3PH_2) = 80$ Torr) (○) and R22 (977.2 cm^{-1}; $E_0 = 1.66$ J per pulse; $P(CH_3PH_2) = 40$ Torr) (□) laser lines of the 00°1–10°0 transition, and P36 (1031.5 cm^{-1}; $E_0 = 1.52$ J per pulse; $P(CH_3PH_2) = 80$ Torr) (◇) and R20 (1078.6 cm^{-1}; $E_0 = 1.67$ J per pulse; $P(CH_3PH_2) = 80$ Torr) (△) lines of the 00°1–02°0 transition (regular pulse) by CH_3PH_2 at ambient temperature.

for by the term $(L/L_0)^a$ (a represents an adjustable parameter). Three constants are also introduced into Eq. (6), namely L_0, T_0 and P_0 (equal to 1 cm, 298 K and 760 Torr respectively) to make the relevant quantities dimensionless.

The applicability of the approach proposed to the description of the absorption data was checked by fitting the experimental characteristics (expressed as OD (Eqs. (1) and (2))) with Eqs. (4)–(6). Primarily, all the data given in Figs. 2, 3, 5, 9 and 10 were simultaneously fitted with the above-mentioned equations, independently for each laser line. Keeping these determined values of the adjustable parameters constant, the absorption data relevant to foreign gases (Figs. 6 and 7) were subsequently fitted with these equations, separately for each gas and laser line. Similarly, the data characteristic of short and long pulses (Figs. 4 and 8) were treated using the primarily determined values of ϵ_0 and E_c and adjusting the values of a, C and n. The calculations were carried out using the least-squares method [32] incorporated in the *Sigma Plot* (Version 5.0) program package. The search for values of the adjustable parameters was repeated several times starting from markedly different initial values to check the stability of the solution with regard to the various parameters. The optimization always converged at the tolerance level 0.00001. The accuracy of the fitted curve can be gauged from the ratio of the standard error of a given parameter to its value. The magnitude of this quantity roughly varied from 0.05 (for ϵ_0) through 0.4 (for E_c and C) to 0.7 (for a and n). This level of accuracy can be considered to be acceptable, taking into account that the number of experimental points was rather limited and the data were gained in markedly different conditions. The latter evaluations demonstrate that Eqs. (4)–(6) present reasonable and optimal analytical expressions for approximating absorption data at high radiation intensity conditions.

The values of the adjustable parameters derived in the above-described manner are listed in Table 1. They are characteristic of a given laser frequency (similar to the absorption of low intensity radiation) and also the temporal distribution of the pulse energy (pulse duration) (we could not see a way to introduce the latter parameter into Eqs. (4)–(6)). One finding is worth mentioning, namely that the powers n and n_i are usually contained in the range 0–1. This may be interpreted to indicate that not all collisions influence the absorption phenomena.

The lines in Figs. 2–10 represent the absorption characteristics calculated by taking the values of the adjustable parameters from Table 1. As can be seen, the conformity of the experimental and theoretical data is quite good, which implies that the phenomenological approach is generally sound. Discrepancies sometimes noted between the experimental and calculated dependences (e.g. in Figs. 2(B) and 10) can be accounted for by experimental uncertainties as well as the

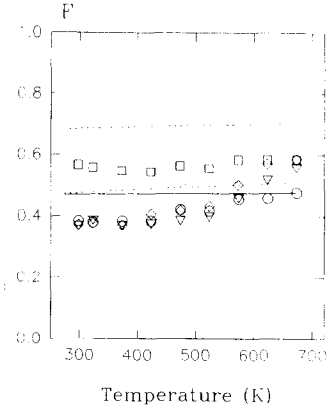

Fig. 10. Fraction of energy absorbed vs. temperature on absorption of the P12 (951.2 cm^{-1}; $E_0 = 1.51$ J per pulse) (○) and R22 (977.2 cm^{-1}; $E_0 = 1.52$ J per pulse) (□) laser lines of the 00°1–10°0 transition, and P36 (1031.5 cm^{-1}; $E_0 = 1.01$ J per pulse) (◇) and R20 (1078.6 cm^{-1}; $E_0 = 1.11$ J per pulse) (△) lines of the 00°1–02°0 transition (regular pulse) by CH_3PH_2 (30 Torr) at 20 cm optical path length.

Table 1
Absorption parameters obtained by approximating the experimental data by Eqs. (4)–(6) [a]

Parameter [b]	00°1–10°0 transition		00°1–02°0 transition	
	P12	R22	P36	R20
	951.2 cm^{-1}	977.2 cm^{-1}	1031.5 cm^{-1}	1078.6 cm^{-1}
ϵ_0	0.00130	0.00304	0.00145	0.00148
E_c	4.35	1.86	0.582	0.755
a	−0.679	−0.105	−0.0321	0.0232
	−0.603 *	−0.221 *	0.128 *	0.200 *
	−0.530 †	−0.540 †	0.00949 †	0.0299 †
$C(CH_3PH_2)$	1.68	1.47	0.805	0.556
	0.763 *	1.75 *	0.454 *	0.250 *
	0.452 †	2.66 †	0.340 †	0.251 †
C(He)	4.96	1.30	2.62	0.705
$C(N_2)$	6.72	1.47	0.828	0.508
$n(CH_3PH_2)$	−0.0722	0.529	0.0555	0.0308
	0.0597 *	0.464 *	−0.0756 *	−0.210 *
	−0.454 †	0.191 †	−0.291 †	−0.347 †
n(He)	0.782	0.835	1.68	0.803
$n(N_2)$	0.929	0.858	0.900	0.435

[a] P_0, L_0 and T_0 were assumed to be 760 Torr, 1 cm and 298 K respectively.
[b] ϵ_0 values in cm^{-1} $Torr^{-1}$; E_c values in J per pulse. Values marked with an asterisk or a dagger correspond to short or long pulses respectively; otherwise to regular (all parameters) or short and long pulses (ϵ_0 and E_c).

limitations of the approach proposed and the optimization procedure used. The particularly pronounced discrepancies observed for the temperature dependence of the fraction of the energy absorbed (Fig. 10) result from the assumption of the specific form of the temperature term $(T/T_0)^{1/2}$ (arising from the kinetic theory of gases). If this term is assumed to be $(T/T_0)^b$ (where b is an adjustable parameter), the correlation between the experimental and calculated dependences improves, but problems with the convergence of the optimization procedure occur.

5. Final remarks

The absorption of CO_2 laser radiation by CH_3PH_2 is characteristic of a given frequency (laser line) and the temporal distribution of the pulse energy. With both of these parameters chosen, the remaining parameters, namely the incident pulse energy, pressure of the absorbing and non-absorbing entities, optical path length and temperature, can be included in the phenomenological relationship (Eqs. (4)–(6); extended form of the Beer–Lambert law) which correctly approximates the experimental data (Figs. 2–10).

Under limiting conditions, Eqs. (4)–(6) reduce to simpler forms. Thus if $E_0 \to 0$, then $\epsilon \to \epsilon_0$, which means that ϵ_0 can be identified with the low intensity, classical absorption coefficient [16]. Accurate absorption coefficients for wavenumbers corresponding to laser lines cannot be extracted from the low resolution IR spectrum shown in Fig. 1 (top graph). Nevertheless, the comparison of low and high intensity spectra (Fig. 1) reveals that the absorption cross-sections increase with decreasing fluence. This effect is also seen in Figs. 2 and 3. Furthermore, if $E_0 \to \infty$, the expression for ϵ is of the form

$$\epsilon_\infty = \epsilon_0 \left(\frac{L}{L_0}\right)^a \left(\frac{T}{T_0}\right)^{1/4} \left\{ C \left[\frac{P}{P_0} \left(\frac{T}{T_0}\right)^{1/4} \right]^n + \sum_i C_i \left[\frac{P_i}{P_0} \left(\frac{T}{T_0}\right)^{1/4} \right]^{n_i} \right\} \quad (7)$$

which reflects the limiting values of the absorption coefficient resulting from an increase in fluence. The approach applied therefore accounts for the features of the absorption phenomena shown in Figs. 2 and 3.

The purpose of these investigations was to obtain the absorption characteristics (F, OD and σ), to determine the parameters influencing these characteristics and to reveal whether a simple analytical expression relating both types of quantities could be found. Eqs. (4)–(6), which satisfactorily approximate the experimental data, have relatively simple forms and include almost all of the parameters affecting the absorption of high power CO_2 laser radiation. They are therefore very convenient for predicting the absorption characteristics and, consequently, the amount of energy absorbed (Eq. (1)) in any experimental conditions. A knowledge of the value of the latter quantity has basic significance in a quantitative description of the photochemistry of the IR region [33,34].

Acknowledgments

Financial support of this work by the Polish State Committee for Scientific Research (KBN) under Grant 2 0679 91 01 (Contract No. 1156/2/91) and by the US Department of Energy under Grant FG02-88 ER 13835 is gratefully acknowledged.

References

[1] J.A. Kaye and D.F. Strobel, *Icarus, 59* (1984) 314.
[2] A.R. Bossard, R. Kamga and F. Raulin, *Icarus, 67* (1986) 305.
[3] J.A. Lannon and E.R. Nixon, *Spectrochim. Acta, Part A, 23* (1967) 2713.
[4] J. Duppre-Maquaire and P. Pinson, *J. Mol. Spectrosc., 62* (1976) 181.
[5] J. Kenne, Y. Ohashi, T. Matsushita, M. Konagai and K. Takahashi, *J. Appl. Phys., 55* (1984) 560.
[6] E. Borsella, L. Caneve, R. Fantoni, S. Piccirillo, N. Basili and S. Enzo, *Appl. Surf. Sci., 36* (1988) 213.
[7] Y.S. Hiraoka, M. Mashita, T. Tada and R. Yoshimura, *Appl. Surf. Sci., 60–61* (1992) 246.
[8] T.F. Deutsch, *Opt. Lett., 1* (1977) 25.
[9] B.G. Gowenlock, P. John, R. Leo, R.G. Harrison, S. Butcher and C. Steel, *J. Photochem., 9* (1978) 200.
[10] F.M. Lussier, J.I. Steinfeld and T.F. Deutsch, *Chem. Phys. Lett., 58* (1978) 277.

[11] J.L. Lyman, R.G. Anderson, R.A. Fisher and B.J. Feldman, *Chem. Phys., 45* (1980) 325.
[12] V. Starov, N. Selamoglu and C. Steel, *J. Am. Chem. Soc., 103* (1981) 7276.
[13] D.K. Evans, R.D. McAlpine, H.M. Adams and A.L. Creagh, *Chem. Phys., 80* (1983) 379.
[14] P. John, M.R. Humphries, R.G. Harrison and P.G. Harper, *J. Chem. Phys., 79* (1983) 1353.
[15] A. Jenichen and H. Johansen, *Z. Phys. Chem. (Leipzig), 265* (1984) 1061.
[16] J. Blazejowski and F.W. Lampe, *J. Photochem., 29* (1985) 285.
[17] E.M. Alonso, A.L. Peuriot and V.B. Slezak, *Appl. Phys. B, 40* (1986) 39.
[18] J. Blazejowski and F.W. Lampe, *Spectrochim. Acta, Part A, 43* (1987) 265.
[19] T. Ristoiu, C. Ungureanu and M. Chirtoc, *Infrared Phys., 29* (1989) 467.
[20] A.M. Robinson and D. Garand, *Appl. Opt., 28* (1989) 967.
[21] L. Giroux, M.H. Back and R.A. Back, *Appl. Phys. B, 49* (1989) 307.
[22] M. Lenzi, E. Molinari, G. Piciacchia, V. Sessa and M.L. Terrenova, *Chem. Phys., 142* (1990) 473.
[23] C.M. Lim, H.J. Kong and S.S. Lee, *J. Opt. Soc. Am. B, Opt. Phys., 10* (1993) 1360.
[24] K.D. Crosbie and G.M. Sheldrick, *J. Inorg. Nucl. Chem., 31* (1969) 3864.
[25] K.W. Saunders and H.A. Taylor, *J. Chem. Phys., 9* (1941) 616.
[26] J.C. Jang and D.W. Setser, *J. Phys. Chem., 83* (1979) 2809.
[27] J. Blazejowski and F.W. Lampe, *J. Appl. Phys., 59* (1986) 2283.
[28] A.M. Robinson, P. Haswell and M. Billing, *Rev. Sci. Instrum., 54* (1983) 117.
[29] M.L. Azcarate and E.J. Quel, *Appl. Phys. B, 47* (1988) 223.
[30] G.P. Quigley and J.L. Lyman, *Springer Ser. Chem. Phys., 6* (1979) 134.
[31] P.W. Atkins, *Physical Chemistry*, W.H. Freeman, New York, 3rd edn., 1986.
[32] D.W. Marquardt, *J. Soc. Ind. Appl. Math., 11* (1963) 431.
[33] J. Blazejowski and F.W. Lampe, *J. Phys. Chem., 93* (1989) 8038.
[34] J. Blazejowski, J. Rak and F.W. Lampe, *J. Photochem. Photobiol. A: Chem., 52* (1990) 347.